THE ASTROPHYSICAL JOURNAL, 520:L131–L134, 1999 August 1

PHYSICAL CONDITIONS IN SHOCKED REGIONS OF ORION FROM GROUND-BASED OBSERVATIONS OF H_2O

JOSÉ CERNICHARO
Instituto de Estructura de la Materia, Departamento de Física Molecular, CSIC, Serrano 121, E-28006 Madrid, Spain; cerni@astro.iem.csic.es
JUAN R. PARDO
California Institute of Technology, MS 320-47, Pasadena, CA 91125
EDUARDO GONZÁLEZ-ALFONSO
Instituto de Estructura de la Materia, Departamento de Física Molecular, CSIC, Serrano 121, E-28006 Madrid, Spain; Universidad de Alcalá de Henares, Departamento de Física, Campus Universitario, E-28871 Alcalá de Henares, Spain
AND
EUGENE SERABYN, THOMAS G. PHILLIPS, DOMINIC J. BENFORD, AND DAVID MEHRINGER
California Institute of Technology, MS 320-47, Pasadena, CA 91125
Received 1999 May 4; accepted 1999 June 1; published 1999 June 23

ABSTRACT

We present observations of the 5_{15}–4_{22} transition of water vapor at 325.15 GHz taken with the Caltech Submillimeter Observatory telescope toward Orion IRc2. The emission is more extended than that of other molecular species such as CH_3OH. However, it is much less extended than the emission of water vapor at 183.31 GHz reported in an earlier paper by Cernicharo and coworkers. A comparison of the line intensities at 325.15 and 183.31 GHz puts useful constraints on the density and temperature of the emitting regions and allows an estimate of H_2O abundance, $x(H_2O)$, of $\simeq 10^{-4}$ in the Plateau and $\simeq 10^{-6}$ to 10^{-5} in the Ridge.

Subject headings: ISM: individual (Orion IRc2) — ISM: molecules — line: profiles — masers — radio lines: ISM — submillimeter

1. INTRODUCTION

Water vapor is an important molecule for the chemistry of interstellar and circumstellar clouds. The 6_{16}–5_{23} masing transition of H_2O at 22 GHz, which arises from levels around 700 K, has been used since its detection by Cheung et al. (1969) to trace high-excitation gas around star-forming regions and evolved stars. The size of the emitting regions at that frequency is typically of the order of a few milliarcseconds (a few times 10^{13} cm). Hence, no information has been obtained from this line on the role of H_2O at large spatial scales. Other H_2O lines have been detected from ground-based or airborne telescopes like the 3_{13}–2_{20} transition at 183 GHz (Waters et al. 1980; Cernicharo et al. 1990, 1994, 1996; González-Alfonso et al. 1994, 1998a), the 4_{14}–3_{21} transition at 380 GHz (Phillips, Kwan, & Huggins 1980), the 10_{29}–9_{36} transition at 321 GHz (Menten, Melnick, & Phillips 1990a), and the 5_{15}–4_{22} transition at 325 GHz (Menten et al. 1990b). Also, the 1_{10}–2_{01} transition of $H_2^{18}O$ at 547 GHz has been observed by Zmuidzinas et al. (1994). Among these lines only the 3_{13}–2_{20} transition at 183 GHz has been used to map the emission of H_2O at very large spatial scale (Cernicharo et al. 1994, hereafter Cer94). The map of the Orion molecular cloud shown in Cer94 is 6 orders of magnitude larger than the size of the spots detected at 22 GHz, and for the first time an H_2O abundance estimate was derived for the different large-scale components of the Orion molecular cloud.

The *ISO* satellite has provided the opportunity to observe thermal lines of water in the middle and far-infrared (see the reviews by van Dishoeck 1997; Cernicharo 1997; and Cernicharo et al. 1997a, 1998). Mapping of the SgrB2 molecular cloud by Cernicharo et al. (1997b) has definitely shown that water vapor is an ubiquitous molecule in molecular clouds with an abundance of 10^{-5}.

Maps of the emission of several H_2O lines in Orion IRc2 have been obtained by Cernicharo et al. (1997a, 1998, 1999). Observations of the central position have been also obtained by van Dishoeck et al. (1998), González-Alfonso et al. (1998b), and Harwit et al. (1998). However, The *ISO* observations of H_2O have drawbacks. In addition to the limited spectral resolution and the high opacity of the thermal lines of H_2O, the poor angular resolution provided by *ISO* in the far-infrared prevents any detailed study of the spatial structure and physical conditions of the H_2O-emitting regions.

An important aid in deriving H_2O abundances could come from the observation of another masing transition of H_2O with similar properties to those of the 183 GHz line.

The 325 GHz line of H_2O was observed by Menten et al. (1990b) in the direction of Orion IRc2 and other molecular clouds. However, no maps were obtained. Here we report the detection of extended water emission at 325 GHz and show that the H_2O abundance is $\simeq 10^{-4}$ in the Plateau. The present data show the importance of ground-based observations of H_2O in deriving the abundance of H_2O in molecular clouds and in providing useful constraints on the physical conditions of the emitting regions. Our ground-based observations provide much finer spatial resolution than *ISO* or *SWAS* and an estimate of $x(H_2O)$ as accurate as that obtained from the extremely optically thick H_2O lines observed in the submillimeter and far-infrared domains.

2. OBSERVATIONS

The observations were performed with the 10.4 m telescope of the Caltech Submillimeter Observatory (CSO) at the summit of Mauna Kea (Hawaii) on 1998 April 1. The receiver, a helium-cooled SIS mixer operating in double-sideband mode (DSB), was tuned at the frequency of the 5_{15}–4_{22} line of H_2O (325.152919 GHz). The H_2O line was placed in the upper sideband (USB) to minimize atmospheric noise from the image sideband (which was at 322.35 GHz). Lines in the signal sideband are severely attenuated relative to those in the image sideband, due to the atmospheric H_2O line. Therefore it was necessary to check the sideband origin of a given line. The

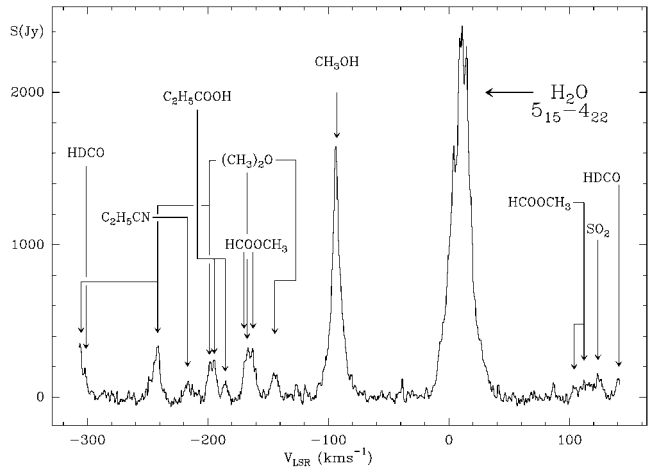

FIG. 1.—Observed spectrum at 325.153 GHz in the direction of Orion IRc2. All lines, except the 5_{15}–4_{22} transition of H_2O and one of the lines of methyl formate (at 100 km s^{-1}), are from the image sideband. The *Y*-axis units are in Jy for the signal sideband. The intensities for the lines in the image sideband are severely overestimated. The 5_{15}–4_{22} line of $H^{18}{}_2O$ at 322.464 GHz (image sideband at V_{LSR} = 100 km s^{-1}) is overlapping with a line of CH_3COOH.

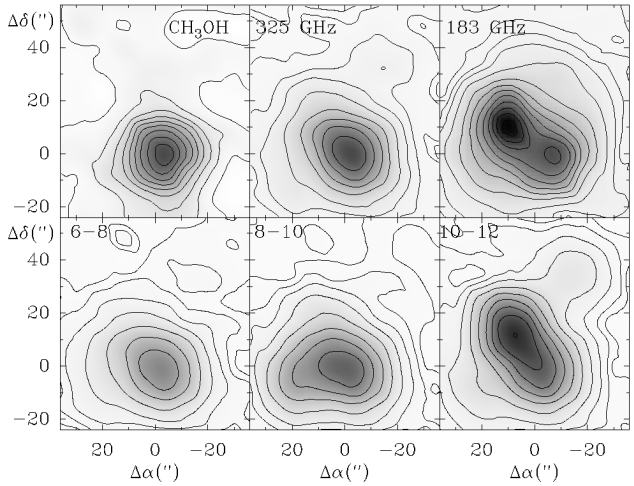

FIG. 2.—Integrated line intensity between −20 and 40 km s^{-1} for CH_3OH (*top left*), H_2O at 325 GHz (5_{15}–4_{22}) (*top middle*), and H_2O at 183 GHz (3_{13}–2_{20}) (*top right*; from Cer94). The CH_3OH data are uncalibrated as the line is in the image sideband. Black contours for H_2O at 325 GHz are 0, 10, 50, 100, and 200–1200 in steps of 200 K km s^{-1}, and for H_2O at 183 GHz they are 100, 300, 600, 1000, and 2000–18,000 in steps of 2000 K km s^{-1}. The other panels show the integrated line intensity of H_2O at 325 GHz for selected velocity intervals (6–8, 8–10, and 10–12 km s^{-1}).

tuning frequency was shifted by 100 MHz to confirm that the central feature in the spectrum of Orion-IRC2 was the water vapor line. The back end consisted of a 1024 channel acousto-optic spectrometer covering a bandwidth of 500 MHz (Δv = 1.1 km s^{-1}). Figure 1 shows the observed spectrum which matches very well the previous observation by Menten et al. (1990b) except for the line intensity (see below).

The pointing was determined by observing the same line toward the O-rich evolved star VY CMa and was found to be accurate to 5″. The weather conditions were very stable during the observations with an atmospheric pressure and temperature of 620 mb and −1.4°C, respectively. The relative humidity was measured to be 4%–5%. The measured opacity from tipping scans at 225 GHz was ≃0.025. During the same night we performed broadband Fourier transform spectroscopy (FTS) measurements of the atmospheric absorption with the FTS described in Serabyn & Weisstein (1995). Model calculations using the multilayer atmospheric radiative transfer model ATM (Cernicharo 1985, 1988; Pardo 1996) yielded an estimated precipitable water vapor column above the telescope of ∼200 μm, which corresponds to a zenith transmission at 325.15 GHz of ∼60% (the corresponding value for the image sideband was ∼87%, hence the line intensities for the image sideband features are overestimated by a factor of ∼2).

The heterodyne H_2O data were calibrated using an absorber at ambient temperature. The calculated system noise temperature, for the signal sideband, was ≃2100 K. The Orion spectrum in Figure 1 shows that the lines from the image sideband are weaker than the 325 GHz H_2O line, i.e., just the opposite of that occurring in the spectrum of Menten et al. (1990b). Rather than a variation of the maser emission (the H_2O line profile in Fig. 1 is identical to that shown in Menten et al. 1990b), we think that this difference is due to much better atmospheric transmission during our observations. We estimate that our intensity scale is correct to within 20%–30%.

The Orion-IRc2 map was carried out in position-switching mode by using the on-the-fly procedure with an off position 5′ away in azimuth. The spatial distribution of the 325 GHz emission is shown in Figure 2 together with that of CH_3OH (from the image sideband) and the 183 GHz emission from Cer94. Integrated intensity maps for selected velocity intervals are also shown in Figure 2.

In order to compare the line profiles of the H_2O lines at 183 and 325 GHz, we reobserved a few positions at 183 GHz with the 30 m IRAM telescope in 1999 January. The weather conditions were also excellent with a zenith opacity at this frequency of ≃1. The spectra, together with those obtained in 1994, are shown in Figure 3.

3. RESULTS AND DISCUSSION

The observed 5_{15}–4_{22} line profile toward the center position looks similar to that of the 3_{13}–2_{20} line observed by Cer94 (see spectra in Fig. 3). However, the antenna temperature of the line is 20 times weaker, and the line profile, although covering the same velocity range, is shifted toward the red. Taking into account the different beam sizes of the IRAM 30 m telescope at 183 GHz and the CSO at 325 GHz, and the extension of the emission in the latter line, we estimate that the main-beam brightness temperature ratio, $R = T_{MB}(183)/T_{MB}(325)$, is 10–20 if both lines were observed with a telescope of 15″ beam size. On the other hand, $T_{MB}(183) \sim 10^3$ K. Both R and $T_{MB}(183)$ are well determined and cannot be related to a calibration problem as the atmospheric conditions were extremely good during our observations at both frequencies. Similar values for R, i.e., R = 10–20, are also found at other positions in the cloud (see Fig. 2) and represent a real difference in the brightness temperatures of the two lines. Only at position $\Delta\alpha = -12''$, $\Delta\delta = 48''$ does the peak temperature of the 5_{15}–4_{22} transition approach that of the 3_{13}–2_{20} transition (the 5_{15}–4_{22} line is, however, narrower). The 325 GHz emission at this position presents a local maximum clearly visible in the velocity maps (see Fig. 2).

Like the 3_{13}–2_{20} line, the 5_{15}–4_{22} transition is masing in nature. There are some narrow features at 325 GHz but with intensities of only a few kelvins, i.e., much weaker than those reported at 183 GHz by Cer94. These features agree in velocity with those found at 183 GHz. However, R changes drastically

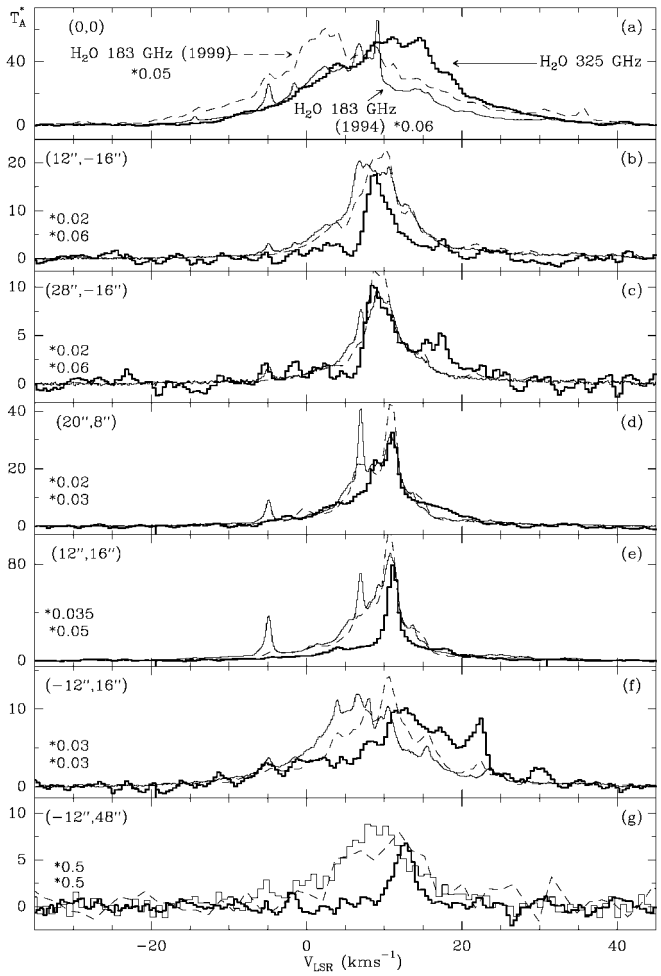

FIG. 3.—Line profiles of the H_2O 5_{15}–4_{22} transition at selected positions (*thick histogram*). The corresponding rescaled data for the 3_{13}–2_{20} line at 183 GHz as observed in 1999 are shown as dashed lines, while those obtained in 1994 are plotted as a solid thin histogram. The scaling factors for the 183 GHz observations (1999 and 1994) are indicated in each panel.

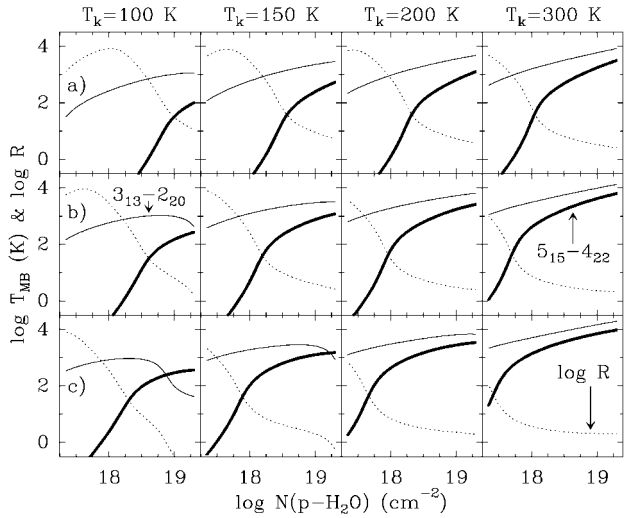

FIG. 4.—Results for the brightness main-beam temperature of the 3_{13}–2_{20} (183.31 GHz) and the 5_{15}–4_{22} (325.15 GHz) transitions vs. the para-H_2O column density. Each column corresponds to a different kinetic temperature (100, 150, 200, and 300 K from left to right), while each row corresponds to a different molecular hydrogen density [$n(H_2) = 3 \times 10^5$, 10^6, and 3×10^6 cm^{-3} correspond to rows a, b, and c].

from feature to feature, a fact that reveals the maser nature of the emission. Outside the central region the lines are very narrow ($\Delta v \simeq 3$–5 km s^{-1}).

Some of the 3_{13}–2_{20} narrow velocity components have antenna temperatures above 2000 K and are probably a few arcseconds in size (Cer94; González-Alfonso 1995). The observations at this frequency performed in 1999 January clearly indicate a variation in the intensity of some of these features with respect to those of Cer94. However, at positions where the line is dominated by the plateau emission ($\Delta\alpha = 28''$, $\Delta\delta = -16''$ and $\Delta\alpha = 12''$, $\Delta\delta = -16''$, for example; see Fig. 3) and outside the central region ($\Delta\alpha = -12''$, $\Delta\delta = 48''$; Fig. 3), the line shape and intensity do not show any significant change between both epochs.

A possible explanation for the 183 GHz and 325 GHz emission being spatially extended could be that it arises from many masing pointlike sources strongly diluted in the beam. This is ruled out by the results of Cer94, where even the strong features at 183 GHz ($T_{MB} \simeq 2000$–4000 K) show an indication of some spatial extent (see above). The densities needed to reproduce the observed brightness temperatures of the maser spots at 22 GHz would result in a thermal or suprathermal 183 GHz line. Consequently, if the 183 GHz emission were arising from the same region than that of the 22 GHz line, very large column densities would be needed to reproduce the observed 183 and 325 GHz intensities. In addition, the weak and extended emission observed at 183 GHz by Cer94 clearly indicates the presence of water vapor coexistent with the molecular gas in the Orion molecular ridge.

In order to understand the behavior of the two masing lines, we have modeled the radiative transfer of the rotational levels of para-H_2O for the physical conditions of the Orion molecular cloud. The radiative transfer method is described in González-Alfonso & Cernicharo (1997), and the model consists of a molecular shell with diameter of 10^{17} cm (size of $15''$ at 450 pc) which expands at a constant velocity of 25 km s^{-1}. Collisional rates between water vapor and helium were taken from Green, Maluendes, & McLean (1993). The helium abundance was assumed to be 0.1, and the rates were corrected to take into account the collisions between H_2O and H_2.

We calculated the statistical equilibrium populations of the lowest 45 rotational levels of para-H_2O for different temperatures ($T_k = 100$, 150, 200, and 300 K), column densities N(para-H_2O), and volume densities [$n(H_2) = 3 \times 10^5$, 10^6, and 3×10^6 cm^{-3}]. Figure 4 shows the main-beam brightness temperatures (T_{MB}) (as observed by a telescope of $15''$ beam size) for the 183 and 325 GHz para-water lines (*thin and thick lines*, respectively), together with R (*dashed lines*). These T_{MB} were computed from the integrated intensity by assuming that the spectral emission is Gaussian shaped.

Inspection of Figure 4 indicates that the line intensity ratio R increases with N(para-H_2O) for low column densities [which depend on T_k and $n(H_2)$]. Both masers are unsaturated in these conditions, but the higher opacity of the 183 GHz transition makes this line more sensitive to variations of N(para-H_2O). For higher values of N(para-H_2O), the 183 GHz line becomes saturated and the exponential amplification of the 325 maser line yields a decrease of R. Finally, when both the 183 and 325 GHz lines are saturated, R approaches a nearly constant value or even decreases below 1 for high $n(H_2)$ and low T_k. The maser at 183 GHz is quenched for these later conditions,

although T_{MB} can still remain above T_k as a result of the suprathermal excitation of the line (see Cer94).

Even for relatively low column densities [$N(\text{para-}H_2O) = 2 \times 10^{17}$ cm^{-2}], low temperatures (100 K), and volume densities (3×10^5 cm^{-3}), the 183 GHz line has an intensity larger than 10 K (see Cer94). However, the possibility of appreciable amplification for the 5_{15}–4_{22} line is much more restricted than for the 183 GHz line, due to the high energy of the levels involved in the 325 GHz line (≈450 K) and to the higher frequency and Einstein coefficient of this transition. This fact explains the difference in spatial extent between both transitions, so that the 325 GHz line is spatially restricted to the Plateau while the 183 GHz line is in addition detected in the Ridge (Cer94).

The water vapor column density that fits the observed $\log R = 1$–1.3 depends strongly on the assumed values of $n(H_2)$ and T_k. The higher $n(H_2)$ and T_k, the lower $N(\text{para-}H_2O)$ that is needed to obtain an appreciable amplification of the 325 GHz line. Figure 4 shows that $R = 10$–20 is obtained in different panels for $N(\text{para-}H_2O)$ ranging from 3×10^{17} cm^{-2} [$n(H_2) = 3 \times 10^6$ cm^{-3}, $T_k = 300$ K] to 2×10^{19} cm^{-2} [$n(H_2) = 3 \times 10^5$ cm^{-3}, $T_k = 100$ K). However, some of these models are not compatible with the observed intensities. For $n(H_2) \geq 10^6$ cm^{-3} and $T_k > 150$ K, we find that $R = 20$ yields $T_{MB}(325)$ in excess of 10^2 K and $T_{MB}(183) > 2 \times 10^3$ K. Both the observed intensities and R are only compatible with more moderate values of $n(H_2)$ and/or T_k. The physical reason is that, for high values of $n(H_2)$ and/or T_k, the collisional pumping of the 183 GHz line becomes so efficient that the emission in this line reaches high intensities for column densities that provide $T_{MB}(325)$ of 50–100 K. Of course, the Plateau may have regions with very high densities and temperatures (which will give rise, for example, to the emission at 22 GHz and to the narrow spectral features observed at 183 and 325 GHz), but these will be much smaller than the observed size of the cloud. The widespread emission from the Plateau we observe at 183 and 325 GHz is compatible only with moderate values of $n(H_2)$ and T_k. In our models, the 22 GHz line will have intensities similar to those already observed in Orion (Genzel et al. 1981) only for the highest kinetic temperatures and volume densities in Figure 4. The brightest spots at 22 GHz could be correlated with the narrow features at 183 GHz and with the relatively weak lines at 325 GHz. Brightness temperatures above 10^6 K can be obtained for large column densities, $T_k > 150$ K, and $n(H_2) > 10^6$ cm^{-3}.

Lower limits for $n(H_2)$ and T_k can be obtained from the observations of other molecular lines (e.g., Blake et al. 1987), so that we adopt $n(H_2) \geq 10^6$ cm^{-3} and $T_k = 100$–150 K. For these conditions we obtain $N(\text{para-}H_2O)$ in the range 2×10^{18}–5×10^{18} cm^{-2}, and hence $N(H_2O)$ in the range 8×10^{18}–2×10^{19} cm^{-2}. The water vapor abundance can be derived from the CO data taken with similar angular resolution (see Cer94). For the intermediate-velocity wind Cer94 derived a CO column density of 10^{19} cm^{-2}. Hence, the $x(H_2O)/x(CO)$ abundance ratio in the Plateau is around 1, i.e., $x(H_2O) \sim (1$–$2) \times 10^{-4}$. In the Ridge molecular cloud the 325 GHz line is very weak. Our models and the 183 GHz data provide an estimate for $x(H_2O)$ of a few 10^{-6} to 10^{-5} (see Cer94), which is in good agreement with our *ISO* results (see Cernicharo et al. 1998, 1999).

The comparison of several masing transitions arising in relatively low energy levels of H_2O allows us to constrain the physical conditions of the different emitting regions. So far, ground-based observations of these transitions with large radio telescopes are the only means to obtain the spatial distribution of H_2O in interstellar clouds.

J. Cernicharo and E. González-Alfonso acknowledge Spanish DGES for this research under grants PB96-0883 and ESP98-1351E. J. R. Pardo gratefully acknowledges the financial support of the Observatoire de Paris-Meudon, CNES, and Météo-France. The CSO is supported by NSF contract AST 96-15025.

REFERENCES

Blake, G. A., Sutton, E. C., Masson, C. R., & Phillips, T. G. 1987, ApJ, 315, 621
Cernicharo, J. 1985, ATM: A Program to Compute Theoretical Atmospheric Opacity for Frequencies Lower than 1000 GHz (IRAM Internal Report 15-April-1992)
———. 1988, Ph.D. thesis, Univ. Paris VII
———. 1997, in Proc. ESA Symp. The Far Infrared and Submillimeter Universe (ESA SP-401; Noordwijk: ESA), 91
Cernicharo, J., González-Alfonso, E., Alcolea, J., Bachiller, R., & John, D. 1994, ApJ, 432, L59 (Cer94)
Cernicharo, J., González-Alfonso, E., & Bachiller, R. 1996, A&A, 305, L5
Cernicharo, J., González-Alfonso, E., & Lefloch, B. 1997a, in Proc. First Workshop on Analytical Spectroscopy (ESA SP-419; Noordwijk: ESA), 23
Cernicharo, J., Thum, C., Hein, H., John, D., Garcia, P., & Mattioco, F. 1990, A&A, 231, L15
Cernicharo, J., et al. 1997b, A&A, 323, L25
———. 1998, in the Proc. ESA Symp. The Universe as Seen by *ISO*, ed. P. Cox & M. Kessler (ESA SP-427; Noordwijk: ESA), in press
———. 1999, in preparation
Cheung, A. C., Rank, D. M., Townes, C. H., Thornton, D. D., & Welch, W. J. 1969, Nature, 221, 626
Genzel, R. Reid, M. J., Moran, J. M., & Downes, D. 1981, ApJ, 244, 884
González-Alfonso, E. 1995, Ph.D. thesis, Univ. Valencia
González-Alfonso, E., & Cernicharo, J. 1997, A&A, 322, 938
González-Alfonso, E., Cernicharo, J., Alcolea, J., & Orlandi, M. A. 1998a, A&A, 334, 1016
González-Alfonso, E., Cernicharo, J., Bachiller, R., & Fuente, A. 1994, A&A, 293, L9
González-Alfonso, E., Cernicharo, J., van Dishoeck, E. F., Wright, C. M., & Heras, A. 1998b, ApJ, 502, L169
Green, S., Maluendes, S., & McLean, A. D. 1993, ApJS, 85, 181
Harwit, M. Neufeld, D. A., Melnick, G. J., & Kaufman, M. J. 1998, ApJ, 497, L105
Menten, K. L., Melnick, G. J., & Phillips, T. G. 1990a, ApJ, 350, L41
Menten, K. L., Melnick, G. J., Phillips, T. G., & Neufeld, D. A. 1990b, ApJ, 363, L27
Pardo, J. R. 1996, Ph.D. Thesis, Univ. Pierre et Marie Curie–Univ. Complutense de Madrid
Phillips, T. G., Kwan, J., & Huggins, P. J. 1980, in IAU Symp. 87, Interstellar Molecules, ed. B. H. Andrew (Dordrecht: Reidel), 21
Serabyn, E., & Weisstein, E. W. 1995, ApJ, 451, 238
van Dishoeck, E. F. 1997, in the Proc. ESA Symp. The Far Infrared and Submillimeter Universe (ESA SP-401; Noordwijk: ESA), 81
van Dishoeck, E. F., Wright, C. M., Cernicharo, J., González-Alfonso, E., De Grauuw, T., Helmich, F. P., & VandenBussche, B. 1998, ApJ, 502, L173
Waters, J. W., et al. 1980, ApJ, 235, 57
Zmuidzinas, J., Blake, G., Carlstrom, J., Keene, J., Miller, D., & Ugras, G. 1994, AAS Meeting, 184, 16.04